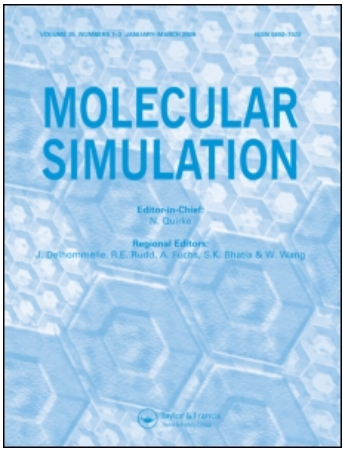

Molecular Simulation
Publication details, including instructions for authors and subscription information:
http://www.informaworld.com/smpp/title~content=t713644482

A Computer Simulation of the Crack Propagation Process

Keisuke Hata[a]; Tadayoshi Takai[b]; Kazumi Nishioka[a]
[a] Faculty of Engineering, University of Tokushima, Tokushima, Japan [b] Faculty of Education, Kagawa University, Takamatsu, Japan

To cite this Article Hata, Keisuke , Takai, Tadayoshi and Nishioka, Kazumi(1991) 'A Computer Simulation of the Crack Propagation Process', Molecular Simulation, 6: 4, 343 — 352
To link to this Article: DOI: 10.1080/08927029108022442
URL: http://dx.doi.org/10.1080/08927029108022442

Molecular Simulation, 1991, Vol. 6, pp. 343–352
Reprints available directly from the publisher
Photocopying permitted by license only

A COMPUTER SIMULATION OF THE CRACK PROPAGATION PROCESS

KEISUKE HATA, TADAYOSHI TAKAI* and KAZUMI NISHIOKA

Faculty of Engineering, University of Tokushima, 2-1 Minamijosanjima, Tokushima 770, Japan
**Faculty of Education, Kagawa University, 1-1 Saiwai-cho, Takamatsu 760, Japan*

(*Received May 1990, accepted August 1990*)

The crack propagation process is studied by Monte-Carlo simulation for a two-dimensional triangular lattice with the Lennard-Jones potential and a surface notch. Nucleation of dislocations at the crack tip and their propagation past the crack tip region are found to precede the crack growth in the present case, this result is in close agreement with that of the molecular dynamics simulation by Halicioglu and Cooper [*Mat. Sci. Eng.*, **79**, 157 (1986)]. To represent the state of the local domain around the crack tip which is characteristic of the onset of dislocation nucleation or that of crack extension, we employ the stiffness coefficients in connection with each atom. It is found that the magnitude of the relevant stiffness coefficient diminishes as each of those processes is about to occur.

KEY WORDS: Crack propagation, Monte-Carlo simulation, dislocation, stiffness coefficient, fracture.

1 INTRODUCTION

Crack propagation is a unique phenomenon among the physical properties of crystals in that the state of a local domain around the crack tip governs the physical behavior, fracture in this case, of the entire system. The state of the local domain in turn is strongly coupled with that of the surrounding material, which makes the phenomenon very complex. Computer simulations on atomic models afford useful tools for gaining insights into the nature of the phenomenon, and numerous studies have been performed as reviewed by Dienes and Paskin [1, 2]. Static or molecular dynamics simulations have been employed so far and the main concerns of the studies have been the comparison of the simulation results with the macroscopic concepts and the theories such as the stress concentration around the crack tip, critical value of the stress intensity factor and the Griffith critical stress.

The present paper aims at gaining information on the characteristic state, which is associated with the crack propagation process, for a local domain around the crack tip. As the variables to represent the state we employ the quantities related to differentials of the potential energy in various orders, i.e., potential energy, interaction force, stress and stiffness coefficients, which are all defined in connection with each atom.

As the model for simulation we employ a two-dimensional triangular lattice with the Lennard-Jones potential, which is the same as that used by Haliciglu and Cooper [3]. They used the molecular dynamics method and found that the crack propagation is preceded by nucleation of dislocation at the crack tip and its propagation past the

crack tip region. The entire process seems to be a thermally activated one, hence the Monte-Carlo method is also expected to work in this case. We employ the Monte-Carlo method in the present work at the same reduced temperature as that chosen by Halicioglu and Cooper [3], and choose the specimen geometry and the loading condition similar to those used by them.

2 METHOD OF CALCULATION

As mentioned already, we use the Monte-Carlo method for simulation in this investigation, and to represent the pair interaction we employ the Lennard-Jones potential

$$u(r_{ij}) = \varepsilon \left\{ \left(\frac{r_0}{r_{ij}} \right)^{12} - 2 \left(\frac{r_0}{r_{ij}} \right)^{6} \right\} \tag{1}$$

with ε and r_0 denoting the energy and the interatomic distance, respectively, at the equilibrium separation for a pair of atoms. r_{ij} denotes the distance between the atoms i and j. The potential energy $\phi(i)$ associated with the i'th atom is given by

$$\phi(i) = \frac{1}{2} \sum_{j \neq i}^{M} u(r_{ij}), \tag{2}$$

where M is the total number of neighbors of the i'th atom confined in a sphere, a circle in the two-dimensional case, of the radius R_{cut}, whose center is at the atom i. R_{cut} is used as the cut-off radius in numerical evaluations. The resultant force $\{F_\alpha(i)\}$ on the atom i from the surrounding atoms is given, for the two-dimensional case, by

$$F_\alpha(i) = \sum_{j \neq i} 12\varepsilon \left\{ \left(\frac{r_0}{r_{ij}} \right)^{6} - \left(\frac{r_0}{r_{ij}} \right)^{12} \right\} \frac{[X_\alpha(j) - X_\alpha(i)]}{r_{ij}^2}, \ (\alpha = 1, 2), \tag{3}$$

where $X_\alpha(j)$ and $X_\alpha(i)$ are the α-components of the position vectors for the i and the j atoms, respectively. The stress components $\{\sigma_{\alpha\beta}(i)\}$ for the atom i are given by

$$v(i)\sigma_{\alpha\beta}(i) = \sum_{j \neq i} 6\varepsilon \left\{ \left(\frac{r_0}{r_{ij}} \right)^{6} - \left(\frac{r_0}{r_{ij}} \right)^{12} \right\} \frac{[X_\alpha(j) - X_\alpha(i)][X_\beta(j) - X_\beta(i)]}{r_{ij}^2}, \tag{4}$$

$$(\alpha, \beta = 1, 2),$$

where $v(i)$ denotes the volume, or the area in the two-dimensional case, associated with the i'th atom, which is defined by the Wigner-Seitz cell surrounding the i'th atom. Although the R.H.S. of Equation (4) is well-defined even for the atoms at the free surface, $\{\sigma_{\alpha\beta}(i)\}$ cannot be defined for those atoms because $v(i)$ cannot be defined for them. For this reason we employ $\{v(i)\sigma_{\alpha\beta}(i)\}$ instead of $\{\sigma_{\alpha\beta}(i)\}$ throughout the present work. The "stiffness coefficients" $\{C_{\alpha\beta\alpha\beta}(i)\}$ for the atom i may be introduced as [4]:

$$v(i)C_{\alpha\beta\alpha\beta}(i) = \sum_{j \neq i} [X_\beta(j) - X_\beta(i)]^2 \left[\frac{6\varepsilon}{r_{ij}^2} \left\{ \left(\frac{r_0}{r_{ij}} \right)^{6} - \left(\frac{r_0}{r_{ij}} \right)^{12} \right\} \right.$$

$$\left. + 2 \times \frac{6\varepsilon}{r_{ij}^4} \left\{ 7 \left(\frac{r_0}{r_{ij}} \right)^{2} - 4 \left(\frac{r_0}{r_{ij}} \right)^{6} \right\} [X_\alpha(j) - X_\alpha(i)]^2 \right], \ (\alpha, \beta = 1, 2), \tag{5}$$

and $\{v(i)C_{\alpha\beta\alpha\beta}(i)\}$ instead of $\{C_{\alpha\beta\alpha\beta}(i)\}$ will be employed in the following due to the

same reason as that stated above. It should be noted that the first term in Equation (5) is absent in the usual formula for a perfect lattice in the mechanical equilibrium [5]. The first term in Equation (5) vanishes also for imperfect lattices if all the atoms are in mechanical equilibrium without the aid of external forces [4].

In all the calculations, R_{cut}, temperature T and ε/k are set to $2.3r_0$, 200 K and 10000 K, respectively, in which k denotes Boltzmann's constant. The cut-off radius of $2.3r_0$ employed here is smaller than the value $3r_0$ which was used by Halicioglu and Cooper [3]. The distance r_{ij} will be normalized with respect to r_0 in the following. In this study, we employ a two dimensional triangular lattice which contains 1791(30×60–9) atoms. A surface notch is created by removing nine atoms from the surface region as shown in Figure 1, where X_1 and X_2 axes are represented by X and Y, respectively, for simplicity. A periodic boundary condition is applied in the X-direction to provide continuity. In the Y-direction, however, two exposed surfaces, one bearing the initial notch, are left intact. One of the close-packed rows is oriented along the X-direction as done by Halicioglu and Cooper [3]. In order to investigate the process of the crack propagation, the system was prestrained uniformly to 8% in the X-direction and the relaxation behavior of the system was examined. When the system was prestrained in the X-direction, the dimension in the Y-direction was uniformly reduced at the same time by considering Poisson's ratio of the perfect lattice. Poisson's ratio was evaluated by extending the perfect lattice in the direction of a close-packed row and numerically evaluating the associated contraction in the perpendicular direction. The value of $8r_0$ was used for R_{cut} for this calculation. Due to the non-linearity of the potential, the value of Poisson's ratio at the state of 8% extension is found to be 0.35753, and this value is used to obtain the initial configuration.

3 RESULTS AND DISCUSSION

Various stages of the crack propagation process are shown as "snap-shots" in Figure 2. The arrangement of atoms shown at each Monte-Carlo step represents that which is obtained by averaging over those of 50 steps following it. This procedure is employed to get the "lattice configuration" by averaging the "thermal fluctuation". The same averaging procedure is employed to obtain the configurations which are used to calculate the quantities given in Figures 4–8. The crack consistently propagates along the close-packed rows in a zig-zag fashion with its overall direction of

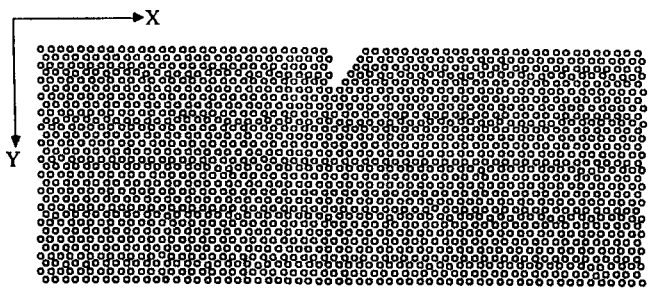

Figure 1 Model for the present simulation.

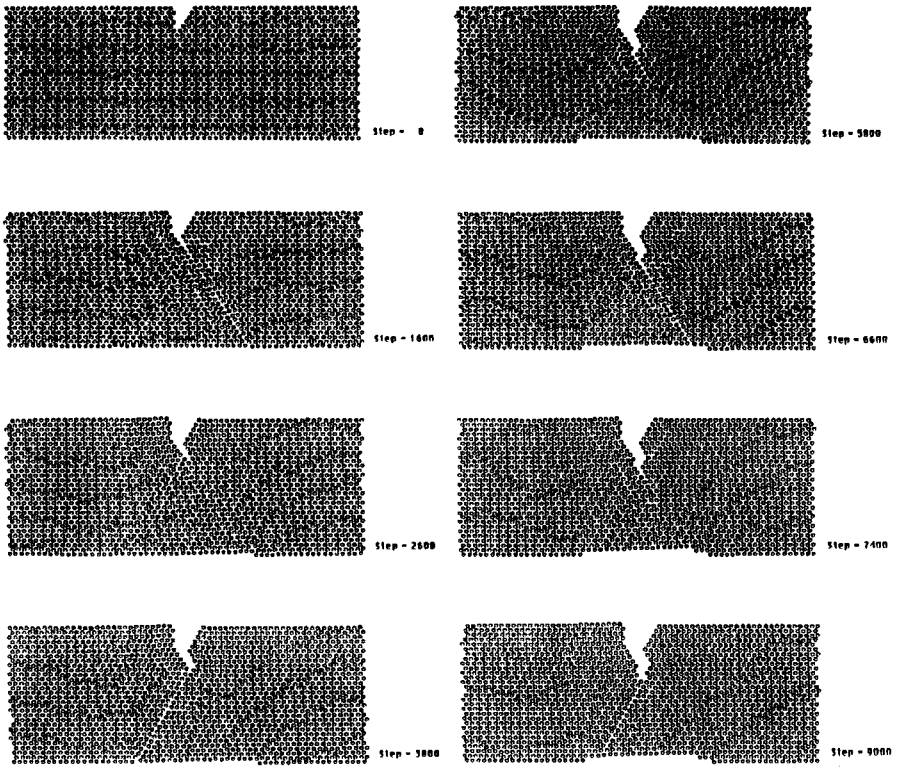

Figure 2 Various stages of the crack propagation process.

propagation approximately perpendicular to the tensile load direction. Before the crack propagates, a slip formation takes place along its line. That is, in this simulation the crack propagation is found to be closely related to nucleation of dislocations from the crack tip and their propagation across the specimen. The behavior of the present system under the 8% prestrain resembles closely to that of Halicioglu and Cooper [3] under the 4% prestrain, and the molecular dynamics and the Monte-Carlo methods are seen to give very similar result in this respect.

The difference of the required prestrains for the crack propagation in the two simulations is considered to be due partly to the variance in the system sizes. Although the number of atomic rows is the same in the two models, the number of columns in the X-direction is 60 in the present model as compared to 80 in the model of Halicioglu and Cooper. The smaller number of columns is expected to require a larger prestrain to result in a similar amount of displacement accumulation around the crack tip during the relaxation process. Another reason for the difference may be due to the variance in the simulation methods. While the motions of all the atoms are determined synchronously hence the cooperative modes of atomic movements are built-in features in the molucular dynamics method, their occurrence is thought to be underrated in the Monte-Carlo method because each atom is moved independently in this case. As a result, the atomic configuration may be trapped in a quasistable state more easily in the Monte-Carlo method than in the molecular dynamics method. Further, a

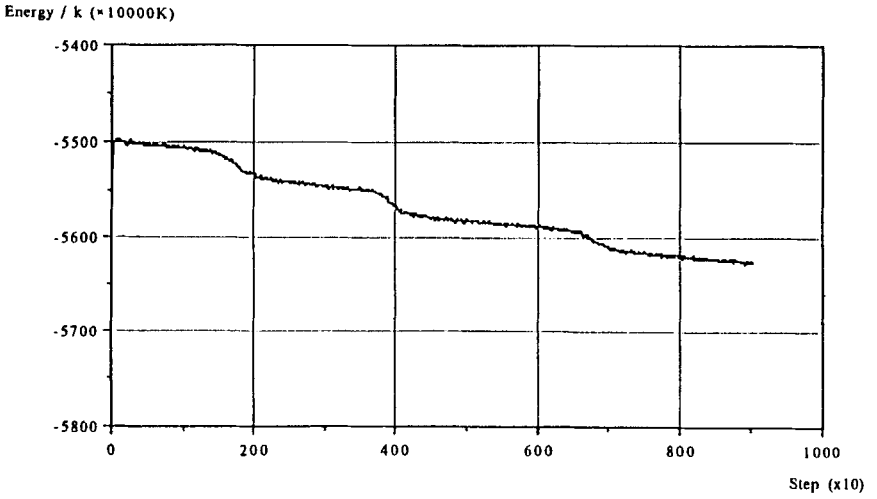

Figure 3 Change of the total potential energy throughout the process.

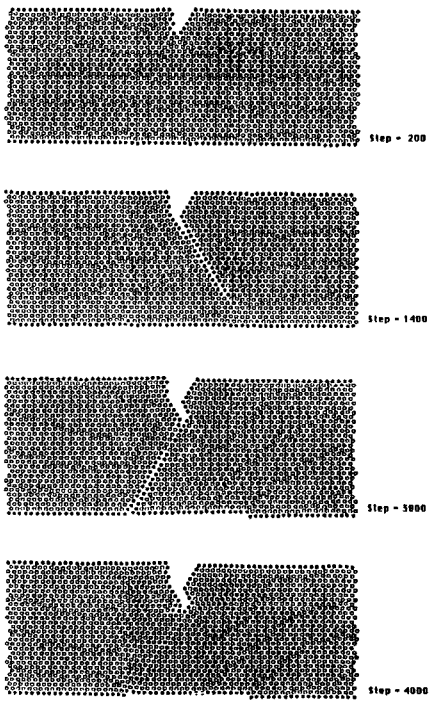

Figure 4 Distribution of the potential energy associated with each atom. Darker symbol designates atoms with the values higher than the border line in Figure 8.

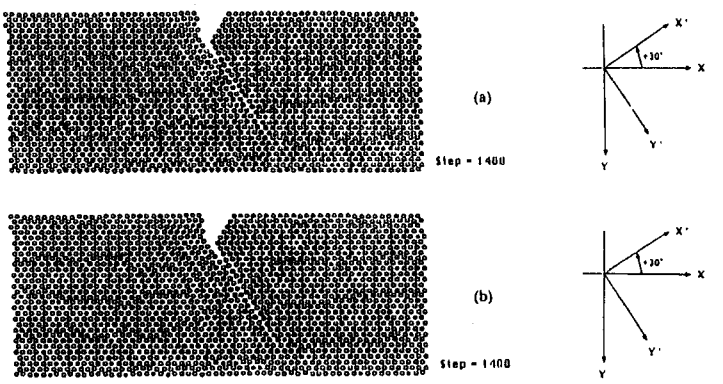

Figure 5 Distribution of the resultant interaction force: (a) $r_0 F_{X'}(i)/k$, (b) $r_0 F_{Y'}(i)/k$. The coordinate axes represented by the suffix are taken along the close-packed rows as indicated by X' and Y'. Darker symbol in $F_{X'}$ designates atoms with the values higher than the border line in Figure 8. Similarly for $F_{Y'}$.

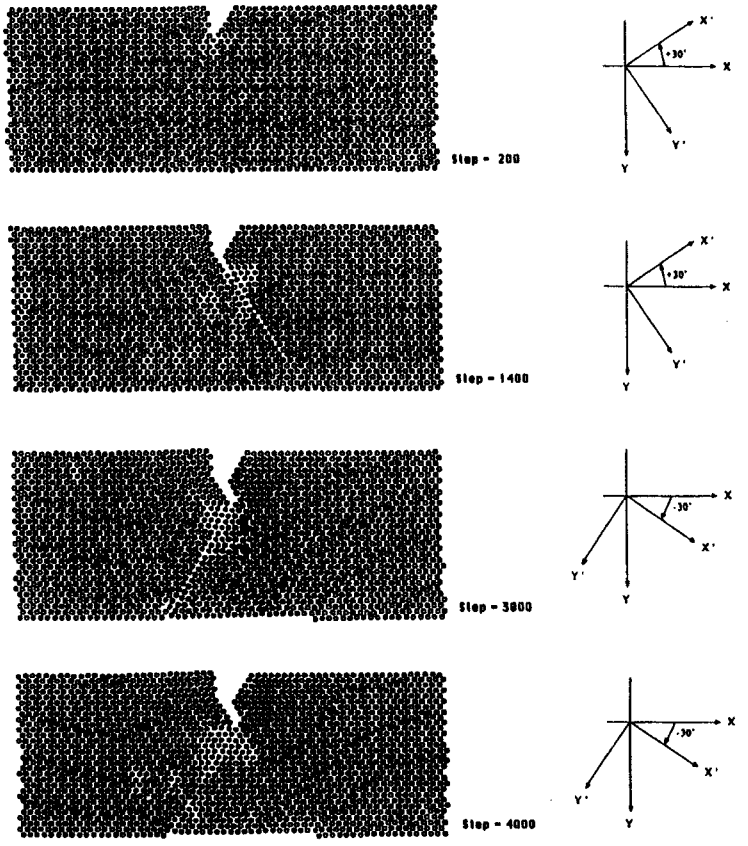

Figure 6 Distribution of $v(i)\sigma_{X'X'}(i)$, where the coordinate axis X' is taken as shown in the figure. Darker symbol designates atoms with the values higher than the border line in Figure 8.

smaller value of the cut-off radius used by the present work may have partially caused to result in the underrated cooperative movements.

The change of the total potential energy throughout the process is shown in Figure 3. As a whole it decreases with the Monte-Carlo step, but the behavior may be classified into the following two categories, i.e., the stages with the steep gradient, which correspond to the nucleation and the propagation of dislocations, and the stages with the gradual change corresponding to the propagation of the crack following the completion of the activity of a dislocation. The gradual character mentioned above is likely to be aided by the creation of the new surface which partially compensates the potential energy release associated with the deformation.

The distributions of the potential energy associated with each atom are shown in Figure 4. Atoms with the values higher than the border line in Figure 8 are designated by the darker symbols. Note that the regions with the higher potential energy are associated with the surface and the core of the dislocations. The distributions of the resultant interaction force are shown in Figure 5, where the new axes X' and Y' are

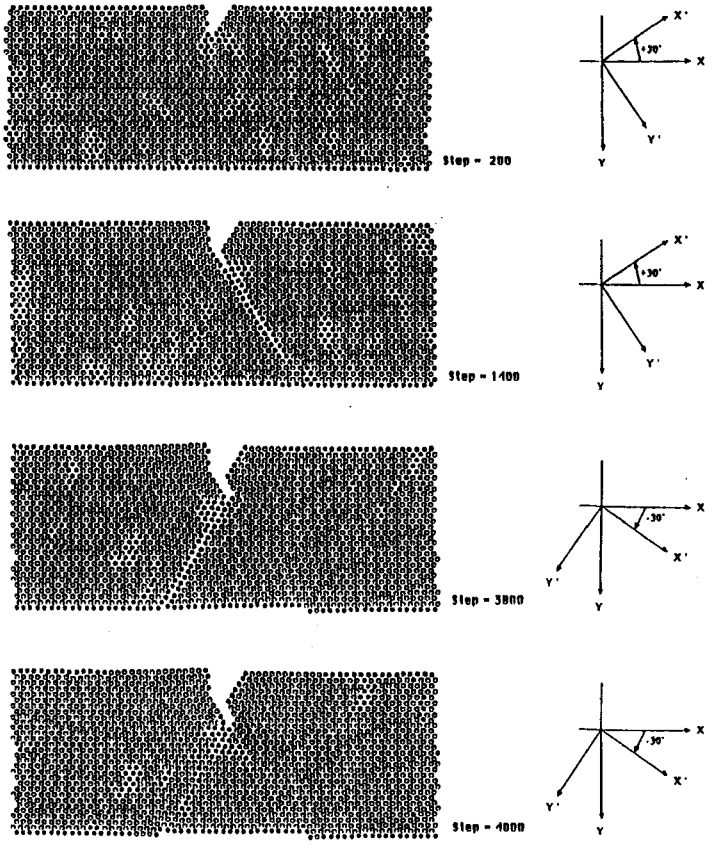

Figure 7 (a) Distribution of $v(i)C_{Y'X'Y'X'}(i)$, where the coordinate axes X' and Y' are taken as shown in the figure. Darker symbol designates atoms with the values lower than the border line in Figure 8.

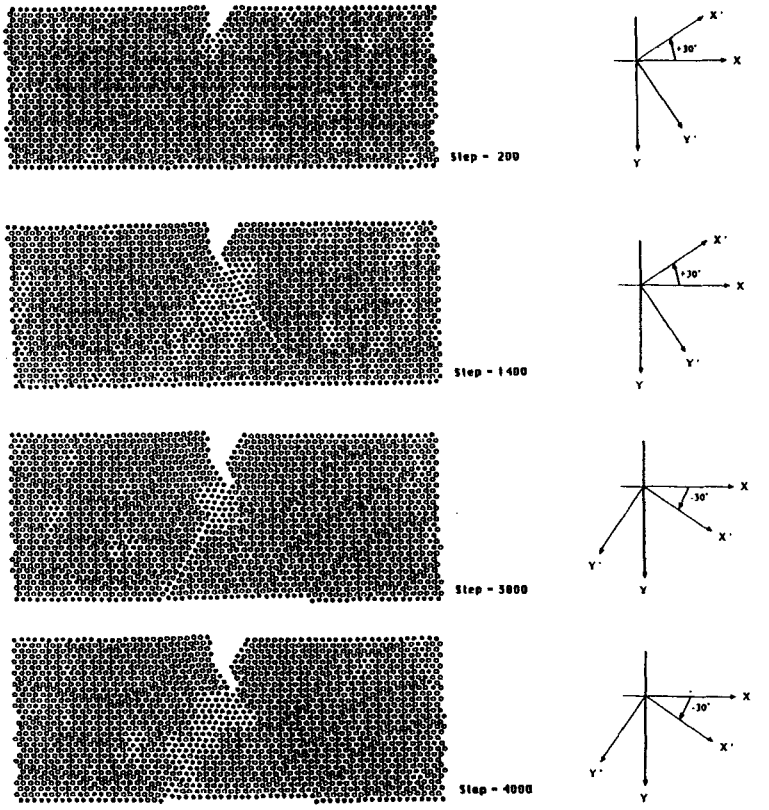

Figure 7 (*Continued*) (b) Distribution of $v(i)C_{X'X'X'X'}(i)$.

introduced as shown in the figure. Atoms with the values higher than the border line in Figure 8, which are shown by the darker symbols, are seen to be randomly distributed. This feature of the distribution of the resultant force remains unchanged throughout the process and is in clear distinction to the other ones shown in Figures 4, 6 and 7, in which the distributions are nonuniform and vary during the process. Thus the resultant force is not a useful variable to represent the characteristic feature of the state around the crack tip. The stress distributions are shown in Figure 6. Atoms with the higher values are again shown by the darker symbols. An inspection of these figures reveals that in all cases the regions with the higher stresses are associated with the crack tip. This result is in good agreement with other works [2, 3, 6]. The distributions of the stiffness coefficients are shown in Figure 7. The atoms with the lower values are designated by the darker symbols in this case. Note that the value of $C_{Y'X'Y'X'}(i)$ is reduced around the line through which a slip formation is about to take place. $C_{Y'X'Y'X'}(i)$ represents the measure for the second order variation of the potential energy, associated with the i'th atom, with respect to the superposition of a homogeneous displacement gradient $\partial w_{Y'}/\partial X'$, where $w_{Y'}$ represents the Y'-com-

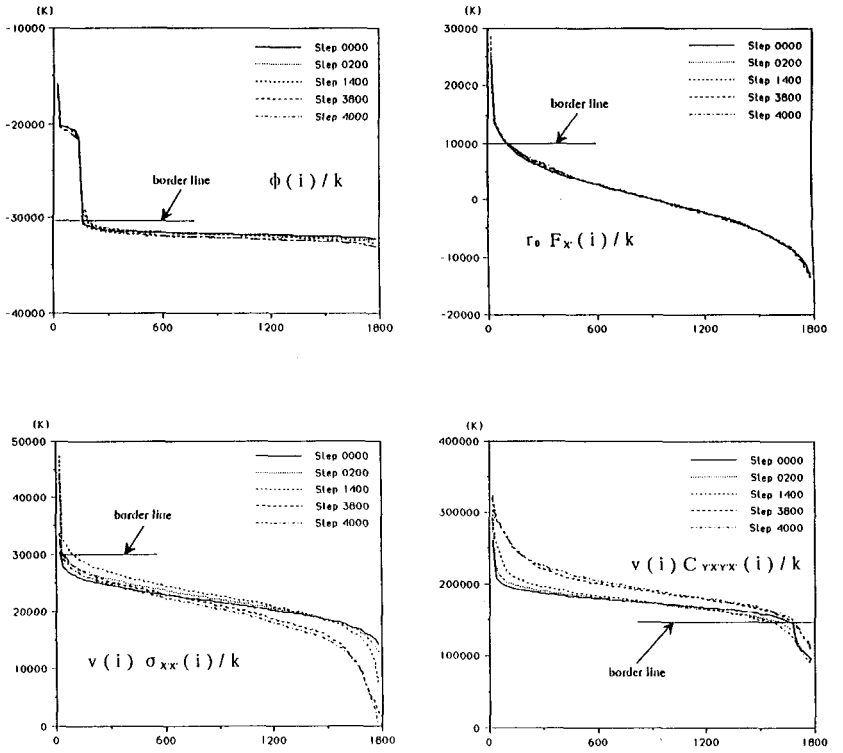

Figure 8 Sorting of the various quantities for each atom according to their magnitudes.

ponent of the displacement vector. Similarly, the value of $C_{X'X'X'X'}$ is reduced at the region where the crack extension is about to take place.

The border lines to determine which atoms are regarded as having the higher or the lower values in Figures 4–7 are given in Figure 8, which displays various quantities for each atom in the order of their magnitudes.

4 CONCLUSION

The following conclusions are obtained from a Monte-Carlo simulation study of crack propagation process for a two-dimensional triangular lattice with the Lennard-Jones potential and having a surface notch.

1) Nucleation of dislocations at the crack tip and their propagation past the crack tip region are found to precede the crack growth in the present case, and this result is in close agreement with that of the molecular dynamics simulation by Halicioglu and Cooper except the difference in the required prestrains for the crack propagation.

2) This difference may be due to the variance in the simulation methods as well as in the system sizes and the cut-off radii employed in those two simulations. However, nothing is conclusive in this respect.

3) Distribution of the stiffness coefficients in connection with each atom seems to

represent the characteristic state of the local domain for the onset of the nucleation and propagation of dislocations and that of the crack extension. Magnitude of the relevant stiffness coefficient at the domain diminishes as each of those processes is about ot occur.

Acknowledgements

The authors wish to thank Mr. K. Shigemura of University of Tokushima for helping them in performing the simulation.

References

[1] G.J. Dienes and A. Paskin, "Computer Modeling of Cracks", in Atomics of Fracture, R.M. Latanision and J.R. Rickens, eds, Plenum, New York, 1983, pp. 671–705.
[2] G.J. Dienes and A. Paskin, "Molecular Dynamic Simulations of Crack Propagation", *J. Phys. Chem. Solids*, **48**, 1015 (1987).
[3] T. Halicioglu and D.M. Cooper, "A Computer Simulation of the Crack Propagation Process", *Mat. Sci. Engineering*, **79**, 157 (1986).
[4] K. Nishioka, T. Takai and K. Hata, "Interpretation of the atomic formulae for the stress and the stiffness coefficients", to be published.
[5] M. Born and Kun Huang, Dynamical Theory of Crystal Lattices, Oxford, 1954, pp. 129–165.
[6] A. Paskin, B. Massoumzadeh, K. Shukla, K. Sieradzki and G.J. Dienes, "Effect of Atomic Crack Tip Geometry on Local Stresses", *Acta Metall.*, **33**, 1987 (1985).